Short Report

Transcriptional explorations of *CAPN3* identify novel splicing mutations, a large-sized genomic deletion and evidence for messenger RNA decay

Mutations in the gene encoding calpain-3 (*CAPN3*) cause autosomal recessive limb-girdle muscular dystrophy type 2A (LGMD2A) and idiopathic eosinophilic myositis. Accurate diagnosis and genetic counselling are based on the identification of disease-causing mutations on both alleles of *CAPN3* in the patients. In the present study, we used transcriptional analysis as a complementary approach for patients suspected of being affected with LGMD2A, in whom initial denaturing high-performance liquid chromatography genomic mutation screening evidenced no or only one *CAPN3* mutation obviously considered as disease causing. This allowed to identify and characterize cDNA deletions. Further genomic analysis allowed to determine the origin of these deletions, either as splicing defects caused by intronic mutations or as an internal multi-exonic deletion. In particular, we report two novel *CAPN3* mutations (c.1745 + 4_1745 + 7delAGTG in IVS13 and c.2185-16A>G in IVS20) and a recurrent large-sized genomic deletion including exons 2–8 for which genomic breakpoints have been characterized. In addition, our results indicate nonsense-mediated messenger RNA decay as a mechanism for under-expression of *CAPN3* associated to some specific variations.

M Krahn[a]*, **C Pécheux**[a]*,
F Chapon[b], **C Béroud**[c],
V Drouin-Garraud[d], **P Laforet**[e],
NB Romero[f], **I Penisson-Besnier**[g],
R Bernard[a], **JA Urtizberea**[h],
F Leturcq[i] **and N Lévy**[a,j]

[a]Département de Génétique Médicale, Hôpital d'enfants de la Timone, Marseille, France, [b]Consultation de Pathologies neuromusculaires et Laboratoire de Neuropathologie, CHU Cote de Nacre, Caen, France, [c]INSERM U827 – Génétique des maladies rares: pathologie moléculaire, études fonctionnelles, banque de données génétiques, Institut Universitaire de Recherche Clinique, Montpellier, France, [d]Service de Génétique, Hôpital Charles Nicolle, Rouen, France, [e]Institut de Myologie and [f]INSERM U582 Institut de Myologie, Hôpital de la Pitié-Salpétrière, Paris, France, [g]Département de Neurologie, CHU, Angers, France, [h]APHP, Hôpital Marin d'Hendaye, Hendaye, France, [i]Laboratoire de Biochimie Génétique, Hôpital Cochin, Paris, France, and [j]INSERM U491, équipe: 'Génétique des maladies neuromusculaires et des Laminopathies', Faculté de Médecine de Marseille, France

*These authors contributed equally to this work.

Introduction

Autosomal recessive limb-girdle muscular dystrophy type 2A (LGMD2A, MIM #253600) and idiopathic eosinophilic myositis are caused by mutations in the gene encoding calpain-3 (*CAPN3*; 15q15.1–15.3) (1–3). Calpain-3 is a non-lysosomal protease mainly expressed in skeletal muscle (4), where it appears to play a central role in sarcomere remodelling (5, 6).

LGMD2A is the most prevalent autosomal recessive LGMD (LGMD2; 10–30%) (7–9). As there is a high clinical variability in patients affected with LGMD2A, calpain-3 protein determination on muscle samples is performed at first instance to orientate diagnosis. However, *CAPN3* mutation analysis is necessary for accurate diagnosis and genetic counselling. Genomic denaturing high-performance liquid chromatography (DHPLC) analysis is particularly adapted for this purpose because of the relatively large size of the gene (24 exons) and the increasing number of reported allelic variants (more than 350 different variants collected in the Leiden Muscular Dystrophy pages database, www.dmd.nl) (10). Unfortunately, in 20–30% of patients, routine genomic analysis fails to identify both disease-causing alleles (10–13). These patients should benefit from complementary approaches towards completing the mutation's identification.

Here, we performed transcriptional analyses in five patients suspected of being affected with LGMD2A, in whom initial DHPLC/genomic mutation screening evidenced no or a single-allele *CAPN3* disease-causing mutation thus not sufficient to firmly confirm diagnosis.

Patients, materials and methods

Patients: inclusion criteria and tissue processing

In the present study, we included five patients for transcriptional analysis of *CAPN3*. Inclusion criteria were (i) diagnosis of LGMD2A suspected on clinical indications of LGMD2, together with a marked decrease or absence of calpain-3 on muscle Western blot analysis; (ii) *CAPN3* genomic mutational screening, identified only one or no mutation clearly identifiable as disease causing (i.e. previously reported as disease causing in the literature or Leiden Muscular Dystrophy pages database, Table 1); and (iii) availability of muscle biopsy samples for transcriptional analysis.

After informed consent, genomic DNA and total RNA were extracted, respectively, from peripheral blood and from frozen muscle tissue obtained from all patients. Approval was obtained from the ethics committees of the institutions involved.

Genomic mutation screening

The 24 exons and flanking intronic boundaries of *CAPN3* were polymerase chain reaction (PCR) amplified, and then analysed using DHPLC as previously described (3, 10).

RNA isolation, complementary DNA preparation, RT-PCR and long-range RT-PCR

Total RNA was extracted from frozen muscle samples with TriPure Isolation Reagent® (Roche, Indianapolis, IN) and reverse transcribed using Superscript II® reverse-transcriptase (Invitrogen, Carlsbad, CA) according to the manufacturer's recommendations. The *CAPN3* complementary DNA (cDNA) coding region was PCR amplified in five overlapping fragments using specifically designed primer pairs (Table S1, conditions and primer sequences available as supplementary material online). Long-range reverse transcriptase–polymerase chain reaction (RT-PCR), covering the coding sequence of exons 1–10, was performed for patient CT5 using primer pairs forward 5′-GCATGCTGCTGGTAGGAGAC-3′/ reverse 5′-CTGAGGGTTGGTCCAGAAAG-3′ (respectively RT1F and RT3R, supplementary material online), with the Expand Long Template PCR System® (Roche) according to the manufacturer's recommendations. RT-PCR products were separated and visualized under ultraviolet light by electrophoresis on 1% agarose gels stained with ethidium bromide.

Bio-informatic analysis

Possible deleterious effects of the identified intronic variants on acceptor splice sites, donor splice sites or splicing branch points were analysed using the Splice Site Finder prediction algorithm (www.UMD.be/SSF). Sorting intolerant from tolerant (SIFT) analysis was done to assess the pathogenicity of the novel missense mutation identified in patient CT1, as described (blocks. fhcrc.org/sift/SIFT.html).

Real-time quantitative RT-PCR

An expression study was performed for patients CT3 and CT4, using two TaqMan® Gene Expression Assays (Applied Biosystems, Foster City, CA): CAPN3 (Assay ID: Hs 00181057_m1) and GAPDH (Assay ID: 99999905_m1) as endogenous expression control. A relative quantification plate was loaded in triplicate with

patient cDNA samples, a normal muscle cDNA sample and a no-template control following the manufacturer's recommendations, and run on a ABI 7500 Real Time PCR System® (Applied Biosystems). Expression levels were obtained by the quantification relative study method, using the normal muscle cDNA sample as calibrator.

DNA and cDNA sequencing

PCR and RT-PCR products were purified using Montage PCR purification Kit® (Millipore, Bedford, MA). For patient CT5, individual long-range RT-PCR bands were gel purified using DNA gel extraction Kit® (Millipore).

PCR and RT-PCR products were sequenced on both strands by use of a terminator procedure, loading on ABI 3130xl Genetic Analyzer® (Applied Biosystems), and analysis using the SEQUENCHER® software (Geno Codes Corporation, Ann Arbor, MI) with comparison to the human *CAPN3* gene sequence (g.DNA # AF209502.1, c.DNA # NM_000070).

Real-time quantitative PCR

A TaqMan® assay (Applied Biosystems) including 5′ FAM-TGACATGTACAAGATCAT-3′ MGB-NFQ as a probe, forward primer 5′-TTTTGA-GATCAGGGATGCTCCTA-3′ and reverse primer 5′-AGCCTCTCTCGATGGCTTTCTT-3′ was designed with PRIMER EXPRESS® software (Applied Biosystems) to amplify a 65 bp amplicon and analyse a target sequence within exon 5 of *CAPN3*. The human serum albumin gene (*ALB*) was used as an internal reference for genomic gene dosage (14).

We carried out multiplex runs in quadruplicate from patient samples, control samples and no-template controls, together with a diploid control for calibration and establishing the comparative threshold cycle curve (ddCT). All reactions were run in 96-well optical plates on a ABI 7500 Real Time PCR System® (Applied Biosystems), using the TaqMan® Universal PCR Protocol and Master mix (Applied Biosystems) according to the manufacturer's recommendations.

Data were analysed with the ABI Prism sequence detection system® (Applied Biosystems) and Microsoft Excel® software (Microsoft, Redmonton, WA). We used the comparative cycle threshold (CT) number method (15) to quantitate the relative copy number ($2^{-(ddCT \pm SD)}$) of the genomic target region (*CAPN3* exon 5) of each unknown sample, relative to the known copy number of the calibrator sample, with

$$ddCT = >[dCtALB - dCTCAPN3]_{\text{calibrator sample}} - [dCtALB - dCTCAPN3]_{\text{unknown sample}}.$$

The ddCT ratios are expected to be close to 1.0 for samples containing two copies of the *CAPN3* genomic target region and close to 0.5 for samples with a hemizygous *CAPN3* allele.

Results and discussion

We used transcriptional analysis in five patients suspected of being affected with LGMD2A, in whom initial DHPLC/genomic mutation screening evidenced no or only one *CAPN3* mutation clearly considered as disease causing. Clinical, muscle biopsy and genomic mutational findings of all patients are presented in Table 1.

Molecular findings in patients CT1, CT2, CT3 and CT4: the intronic variants c.2185-16A>G, c.1745 + 4_1745 + 7delAGTG and c.802-9G>A cause abnormal splicing of the CAPN3 messenger RNA

Patient CT1
Genomic mutation screening identified a novel missense mutation (c.1259C>A; p.Ala420Asp, exon 10, not found in 200 control chromosomes), predicted as non-tolerant substitution using SIFT analysis (SIFT score 0.01). In addition, a novel intronic variant, c.2185-16A>G (IVS20) (Table 1 and Fig. S1, supplementary material online), was identified. Both mutations have also been identified in the two symptomatic sisters of the patient (16).

cDNA analysis confirmed the missense change (r.1259C>A) and identified a deleterious effect of c.2185-16A>G: a heterozygous in-frame insertion of 15 bp from IVS20 located immediately 5′ from the splice acceptor site (Table 2), and predicted to cause an insertion of five amino acids (p.Gln728_Lys729insIlePheTyrCysGln) in domain IV of calpain-3 (implicated in calcium binding and homo-dimerization (17)). In regard to the complete absence of calpain-3 on Western blot analysis, we conclude that this amino acid insertion destabilizes the protein. To our knowledge, this constitutes the first reported case of an isolated calpain-3 amino acid insertion.

Patient CT2
At the genomic level, a novel 4 bp intronic deletion in IVS13, c.1745 + 4_1745 + 7delAGTG, was found, together with c.1746-20C>G (10, 12, 16, 18) (Table 1 and Fig. S1, supplementary material online).

cDNA analysis evidenced the deleterious effect of c.1745 + 4_1745 + 7delAGTG as an in-frame

Table 1. Resume of clinical, pathological, and *CAPN3* genomic mutational data of the patients included in this study

Patient	Clinical findings	Muscle biopsy findings	Genomic mutational findings (DHPLC and sequence analysis)
CT1	Pelvic and shoulder girdle weakness at the age of 45 years, rapidly leading to difficulties in rising from chairs, climbing stairs and walking. At clinical examination, scapular winging, upper and lower limb proximal weakness with thigh amyotrophy, and hyperlordosis. No evidence of distal involvement. Moderate impairment of respiratory functions (but current smoker, 4 cigarettes/day). Involvement of the facial muscles, with difficulties closing his eyes, and dysarthria (initial diagnostic suspicion of facio-scapulo-humeral dystrophy, but no deleted D4Z4 allele was identified). Muscle computed tomography scan examination: proximal involvement of the lower limbs, predominating at the posterior compartment, and the upper limbs, with the biceps brachii being severely affected	Dystrophic pattern, with normal immunostaining using antibodies against dysferlin, caveolin-3 and the sarcoglycan complex. Complete absence of calpain-3 bands p94, p60, and p30 on Western blot analysis	Exon 10: c.1259C>A (p.Ala420Asp), heterozygous, not previously reported; and IVS20: c.2185-16A>G (abnormal splicing), heterozygous, not previously reported
CT2[a]	Difficulties in running during childhood, which evolved to an abnormal gait. Diagnosis of myopathy first evoked at the age of 35 years with predominant proximal weakness of the lower limbs. Subsequent weakness of the shoulder girdle at the age of 60 years. At the age of 77 years: scapular winging, upper and lower limb proximal weakness, and calf hypertrophy. No distal deficiency, cardiomyopathy, involvement of the facial muscles or impairment of the respiratory function. Invalidating limb-girdle muscular dystrophy. Detailed clinical information not available	Marked variation in fibre size and lobulated fibres, but no signs of necrosis–regeneration. Severe decrease of calpain-3 bands p94, p60, and p30 on Western blot analysis	IVS13: c.1745 + 4_1745 + 7delAGTG (abnormal splicing), heterozygous, not previously reported; and IVS13: c.1746-20C>G, heterozygous, previously reported, pathogenicity unlikely (10, 12, 16, 18, 25).
CT3	Detailed pathological data not available.	Severe decrease of calpain-3 bands p94, p60, and p30 on Western blot analysis	IVS5: c.802-9G>A (abnormal splicing, NMD), heterozygous, previously reported (3, 12, 16); and Exon 13: c.1714C>T (p.Arg572Trp), heterozygous, previously reported (9, 11, 12, 16, 19, 20).

Table 1. Continued

Patient	Clinical findings	Muscle biopsy findings	Genomic mutational findings (DHPLC and sequence analysis)
CT4[a]	Evolving moderate proximal weakness of the upper and lower limbs since the age of 13 years. At the age of 16 years: elbow and aquilae retraction and spine stiffness with associated kyphosis. No distal deficiency, cardiomyopathy, involvement of the facial muscles or impairment of the respiratory function	Dystrophic changes with marked variation in fibre size and presence of necrotic fibres. Rare inflammatory foci mainly composed of macrophages and eosinophils were noted. Normal immunostaining using antibodies against spectrin beta, laminin, emerin, and the sarcoglycan complex. Irregular immunostaining for dysferlin, some fibres being not stained, whereas others present an irregular peripheral staining, with or without sarcoplasmic staining. Complete absence of the calpain-3 bands p94, p60, and p30 on Western blot analysis	IVS5: c.802-9G>A (abnormal splicing, NMD), heterozygous, previously reported (3, 12, 16); and IVS22: c.2380 + 12delA, homozygous, previously reported, pathogenicity unlikely (3, 9, 12, 13, 16).
CT5	Difficulties since she started walking, initially with clumsiness at tiptoe walking, then proximal weakness of the upper and lower limbs, with moderate winging of the scapulae, elbow and aquilae retraction and hyperlordosis. No facial involvement. At the age of 21 years: slowly evolving difficulties in rising from chairs and climbing stairs	Marked variation in fibre size, interstitial fibrosis and presence of rare necrotic fibres. Complete absence of the calpain-3 bands p94 and p60 (p30 not tested) on Western blot analysis	Exon 11: c.1373delC (p.Pro458LeufsX5), heterozygous, previously reported (9, 16, 26).

NMD, nonsense-mediated messenger RNA decay.
[a]In patients CT2 and CT4, only one disease-causing mutation could be identified using a combined approach of genomic mutational screening and cDNA analysis. As these patients present, respectively, a severe decrease and an absence of calpain-3 bands on Western blot analysis (excluding a secondary calpain-3 deficiency), diagnosis of primary calpainopathy is most likely. Both patients may carry a second disease-causing mutation, which could not be identified using this combined approach (i.e. a non-identified large genomic rearrangement).
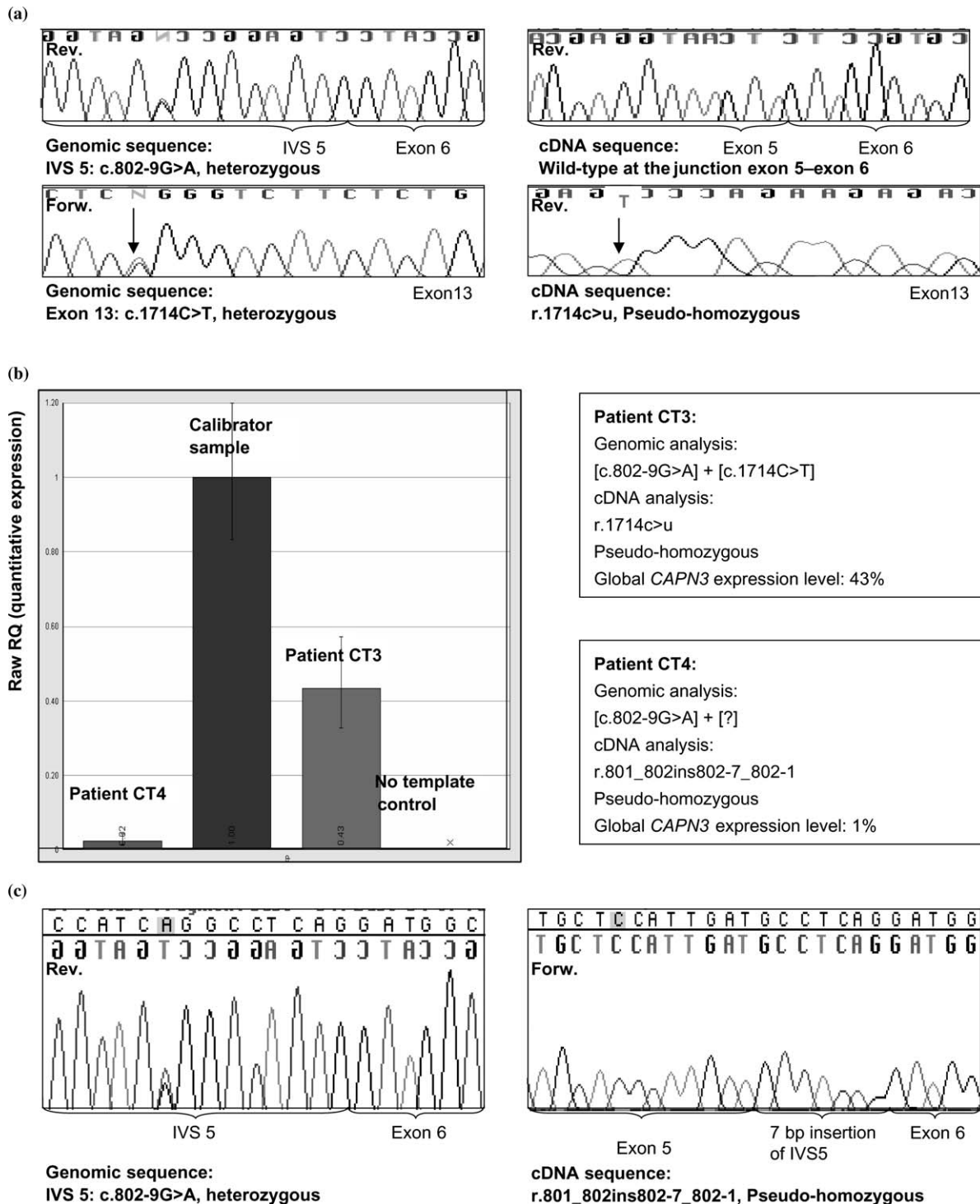
Fig. 1. Analysis of the deleterious effect caused by the c.802-9G>A mutation evokes nonsense-mediated messenger RNA decay. (**a**) Genomic and complementary DNA (cDNA) sequence analysis in patient CT3. (**b**) Global *CAPN3* expression analysis in patients CT3 and CT4 using quantitative reverse transcriptase–polymerase chain reaction. (**c**) Genomic and cDNA sequence analysis in patient CT4. Forw., forward sequence; Rev., reverse sequence.

deletion, removing 87 bp from the terminal 3′ part of exon 13, possibly by activating a cryptic splice site. This is predicted to delete 29 amino acids (p.Tyr554_Glu582del) in domain III of calpain-3.

A possible deleterious effect of c.1746-20C>G has been initially evoked (12, 16). In patient CT2, cDNA analysis did not show any sequence variation in the region of exon 14 (i.e. insertions and/or deletions), which could have resulted from

abnormal splicing possibly caused by this variant (data not shown). This is concordant with recent data (18) and argues against a deleterious effect.

Patients CT3 and CT4

In both patients CT3 and CT4, genomic analysis identified the mutation c.802-9G>A (IVS5) at a heterozygous state (Table 2).

In patient CT3, a missense mutation (exon 13: c.1714C>T; p.Arg572Trp) (9, 11, 12, 16, 19, 20) was identified in *trans*. Whereas patient CT3 is compound heterozygous [c.802-9G>A] + [c.1714C>T] at the genomic level, cDNA analysis retrieved only the c.1714C>T mutation (pseudo-homozygous state) (Fig. 1a). Therefore, c.802-9G>A may cause nonsense-mediated messenger (mRNA) decay (NMD) or a linked phenomenon in this patient because pseudo-homozygous mutations at the mRNA level as compared with the genomic findings may evoke this mechanism (21). According to a mono-allelic expression, quantitative reverse transcriptase–polymerase chain reaction (QRT-PCR) with a TaqMan® probe showed a global level of expression of 43% (Fig. 1b). NMD has recently been shown to occur for nonsense and frameshift *CAPN3* mutations (18). We here show the possible existence of NMD caused by an intronic variant, most likely by causing abnormal splicing and subsequent introduction of a premature termination codon.

In patient CT4, the c.802-9G>A mutation was found heterozygous. In addition, the c.2380 + 12 delA variant (16) was found at a homozygous state, without any qualitative effect at the cDNA level (no sequence variation in the region of exons 22 and 23).

Surprisingly, the effect of the c.802-9G>A variant in patient CT4 differed from the findings in patient CT3: we observed a pseudo-homozygous insertion of 7 bp from IVS5 located immediately 5′ from the splice acceptor site (Fig. 1c), most likely because of the activation of a cryptic splice acceptor site. This causes a frameshift introducing a premature translation stop codon >50 nucleotides upstream of the last exon–exon junction and thus candidate for NMD (22). QRT-PCR with a TaqMan® probe showed a global level of expression reduced to 1% (Fig. 1b). Therefore, the pseudo-homozygous r.801_802ins802-7_802-1 insertion in patient CT4 could be related to a non-identified mutation in *trans*, leading to a 'complete' absence of the resulting mRNA (i.e. a non-identified large genomic rearrangement, mutations in the promoter region, etc.). This would explain that, even if the majority of mRNA originating from the c.802-9G>A allele is subject to NMD, a residual amount of r.801_802ins 802-7_802-1 mRNA is observed in this patient.

In addition, the different findings in patients CT3 and CT4 could be partially caused by inter-individual variation in NMD efficiency (23, 24), related to yet unexplained genetic modifying factors.

Bio-informatic splice site analysis

All intronic variants identified in this study were analysed using Splice Site Finder, a novel algorithm for the prediction of deleterious effects on normal splicing. All bio-informatic predictions are concordant with the results of cDNA analysis (Table 2 and Fig. 3a).

Molecular findings in patient CT5: characterization of a large-sized genomic deletion including exons 2–8

Genomic DHPLC screening identified a heterozygous frameshifting mutation in exon 11 (c.1373 delC) (Table 1), but no additional variant. Accordingly, this mutation was retrieved heterozygous in her mother, whereas no mutation was identified in her father (non-paternity excluded using microsatellite analysis). cDNA analysis retrieved the c.1373delC mutation but no additional sequence variant.

To test the hypothesis of a large-sized deletion or abnormal splicing pattern, we used long-range RT-PCR with a set of primers amplifying the entire cDNA (data not shown) and a set amplifying exons 1–10, which amplified three bands (Fig. 2a): one of the expected size (~1650 bp) and two additional bands of ~850 and ~550 bp. Sequencing of the additional bands after gel purification (Fig. 2a) showed two abnormal transcripts: (i) one with a deletion from exons 2–8 (r.310_1115del, p.Glu104_Arg372delfsX11, deletion of 806 bp, corresponding to the band of ~850 bp = ~1650 bp − 806 bp) and (ii) a second with the same deletion and, in addition, a deletion of 321 bp within exon 1, flanked by a 5′-GT dinucleotide, a 3′-AG dinucleotide, including 52 bp of the 5′UTR and the initial 269 coding base pairs of exon 1 ([r.-52_269del; r.310_1115del] corresponding to the band of ~550 bp = ~1650 bp − 806 bp − 321 bp).

The large-sized genomic deletion including exons 2–8 (r.310_1115del, Fig. 3b) has been previously reported (Fig. 3c) (16, 27, 28) but not characterized at the genomic level.

Therefore, we next used genomic quantitative PCR with a TaqMan® probe located in exon 5 (Fig. 2b). In a diploid control population of four healthy male and five healthy female individuals,

Table 2. Effect of intronic sequence variants identified in this study: bio-informatic analysis of possible deleterious effects and results of complementary DNA analysis

Intronic sequence variant (genomic DHPLC and sequence analysis)	Wild-type sequence[a]	Mutant sequence[a]	Predicted consequence	cDNA analysis
IVS5: c.802-9G>A, previously reported (3, 12, 16)	attctccatc**g**ggc, CV = 60.8	attctccatc**a**ggc, CV = 89.8	Creation of an alternative acceptor splice site that results in a frameshift (+8 nucleotides) and could lead to nonsense-mediated messenger RNA decay (wild-type site CV = 85.4). Pathogenic mutation	Undetectable allele (patient CT3) r.801_802ins802-7_802-1 (patient CT4)
IVS13: c.1745 + 4_1745 + 7delAGTG, not previously reported	TGAgtg**agtg**, CV = 81.43	TGAgtg---ctg, CV = 58.4	Inactivation of the donor splice site. Activation of the closest alternative donor splice site and deletion of 87 nucleotides (CGAGTACGT, CV = 75.8) Pathogenic mutation	r.1659_1745del (patient CT2)
IVS13: c.1746-20C>G, previously reported (10, 12, 16, 18, 25)	ctgagaccccac**a**t, CV = 54.37	ctgagaccccag**a**t, CV = 83.3	Creation of an alternative acceptor splice site that overlaps the branch point and is therefore not used (note that the branch point motif is not affected by the mutation) Non-pathogenic variation	No abnormality identified (patient CT2)
IVS20: c.2185-16A>G, not previously reported	gacctccatc ctca**a**attt ctattgccag AAA, CV = 60.2	gacctccatc ctca**g**attt ctattgccag AAA, CV = 89.2	Creation of an alternative acceptor splice site and insertion of 15 nucleotides (wild-type site, CV = 88.1) Pathogenic mutation	r.2184_2185ins2185-15_2185-1 (patient CT1)
IVS22: c.2380 + 12delA, previously reported (3, 9, 12, 13, 16)	No impact on splice sites	No impact on splice sites	Non-pathogenic variation	No abnormality identified (patient CT4)

[a]Affected nucleotides are in bold and underlined, exonic nucleotides are capitalized. Consensus value (CV) >70 = possible active splice sites; CV <70 = inactive splice sites.
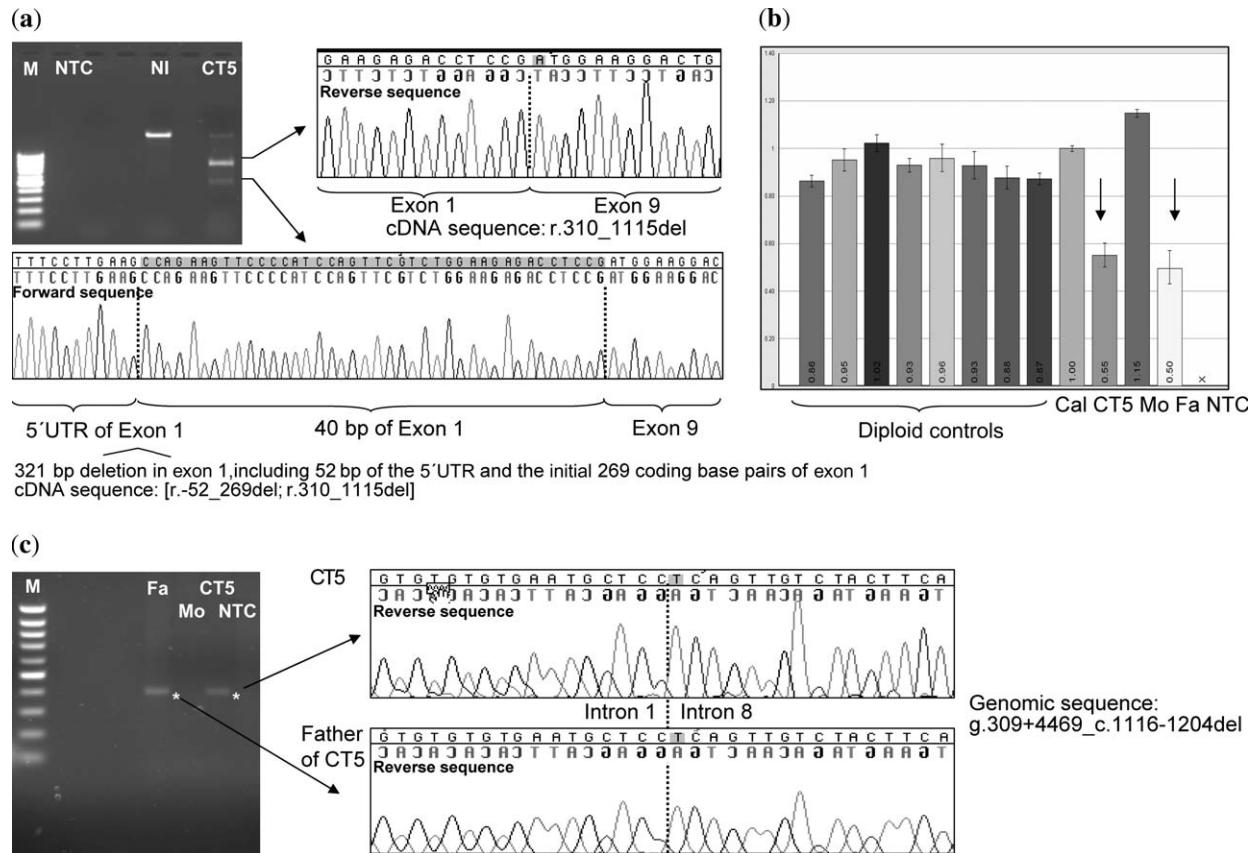
589

(a)

(b)

(c)

Fig. 2. Characterization of a *CAPN3* large-sized genomic deletion including exons 2–8. (a) Long-range reverse transcriptase–polymerase chain reaction using primers RT1F and RT3R, and sequencing of the two additional bands (arrows) in patient CT5, revealing a deletion of exons 2–8. (b) Genomic quantitative polymerase chain reaction (PCR) with a TaqMan® probe located in *CAPN3* exon 5: comparative threshold cycle curve ratios and SD of nine healthy control individuals, patient CT5 and her parents; note the hemizygous state for the patient and her father (arrows). (c) Identification of a genomic PCR junction fragment (*) in patient CT5 and her father, and sequencing of the genomic borders/breakpoints of the deletion. CT5, patient CT5; Fa, father of patient CT5; Mo, mother of patient CT5; Nl, normal control; M, 100 bp ladder; Cal, calibrator sample; NTC, no-template control sample.

the ddCT ratio ranged from 0.86 to 1.02. A ddCT ratio of 1.15 (diploid) was found for the patient's mother, whereas the patient and her father were found hemizygous (respective ddCT values of 0.55 and 0.50), thus confirming the hypothesis of a large-sized genomic deletion in the patient, inherited from her father.

We determined the genomic borders/breakpoints of this deletion using long-range PCR. A ~6 kbp junction fragment was first obtained in the father of the patient (with a forward primer located 5′ of exon 1 and a reverse primer located 3′ of exon 9, data not shown). We sequenced this junction fragment, and then 'walked' with internal primers. One particular reverse primer (5′AATGGGTTCTGGACATAGACA3′) in IVS8 revealed the genomic junction. This was further confirmed in the patient with internal/nested primers (forward 5′GACCAGCA-CATGGTTGAGTG3′ and reverse 5′GAT-GCAGCAAAGGGAATCTC3′), amplifying a shorter PCR junction fragment (Fig. 2c). Sequencing of this fragment confirmed the genomic junction joining IVS1 to IVS8 (g.309 + 4469_c.1116-1204del) (Fig. 2c).

This deletion was neither retrieved in patients CT2 and CT4 nor in 18 additional patients suspected of being affected with LGMD2A, for whom only one or no *CAPN3* mutation had been identified and for whom no muscle tissue was available for cDNA analysis. However, as this deletion has been previously reported in three patients (16, 27, 28), it should be interesting to evaluate whether it constitutes a recurrent mutation or an ancestral mutated allele.

Some possible LGMD2A patients with only one or no identified *CAPN3* disease-causing mutation may carry partial *CAPN3* gene deletions or duplications. In particular, in this study, cDNA analysis in patients CT2 and CT4 obviated,
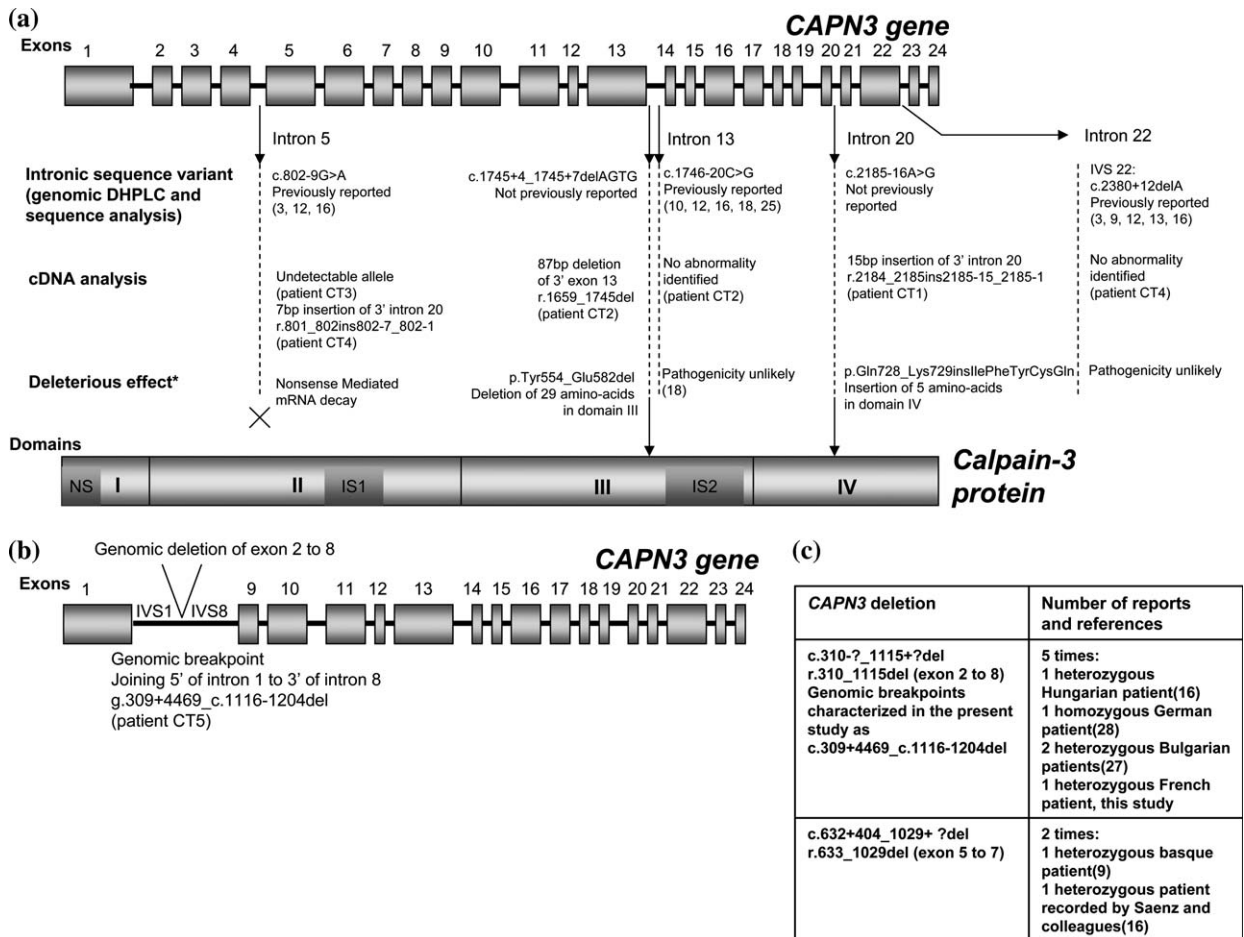
Fig. 3. (**a**) Effect of intronic variants, identified at the complementary DNA (cDNA) level in this study. (**b**) Consequence of the large-sized deletion at the genomic level. (**c**) Large exonic deletions described in the *CAPN3* gene. Representation of introns is not to scale. *Effects on the amino acid sequence are predicted from the cDNA sequence.

respectively, only one clearly pathogenic mutation. A large genomic rearrangement in *trans*, but different from the deletion identified in patient CT5, is a hypothesis to be further evaluated. To date, no exonic duplications and only two different exonic *CAPN3* deletions have been identified (Leiden Muscular Dystrophy pages database (9, 16, 25–27) (Fig. 3c), probably because routine mutation detection techniques (i.e. single strand conformation polymorphism analysis, DHPLC or direct sequencing) cannot detect large genomic rearrangements. Our report further illustrates the existence of large exonic *CAPN3* deletions. Genomic rearrangements may be identified by cDNA analysis (i.e. deletions of one or several exons), leading to an orientated genomic analysis (9). However, a more systematic approach using quantitative multiplex PCR of short fluorescent fragments (28) and/or multiplex ligation-dependent probe amplification (29) should be developed for more cost-effective and routine-based screening.

For exhaustive mutational screening in LGMD2A patients, a combinatory genomic and transcriptional approach should ideally be used and allow for the detection of both disease-causing mutations in most patients (including novel intronic mutations and large genomic rearrangements), accurate diagnosis and genetic counselling.

Supplementary material

Table S1. RT-PCR conditions, primer pairs and amplified regions of the *CAPN3* cDNA used in this study.
Fig. S1. CAPN3 muscle cDNA sequencing in patients CT1 and CT2. Forw, forward sequence; Rev, reverse sequence.
Supplementary materials are available as part of the online article at http://www.blackwell-synergy.com/.

Acknowledgements

References

1. Chiannilkulchai N, Pasturaud P, Richard I, Auffray C, Beckmann JS. A primary expression map of the chromosome 15q15 region containing the recessive form of limb-girdle muscular dystrophy (LGMD2A) gene. Hum Mol Genet 1995: 4: 717–725.

2. Richard I, Broux O, Allamand V et al. Mutations in the proteolytic enzyme calpain 3 cause limb-girdle muscular dystrophy type 2A. Cell 1995: 81: 27–40.

3. Krahn M, Lopez de Munain A, Streichenberger N et al. CAPN3 mutations in patients with idiopathic eosinophilic myositis. Ann Neurol 2006: 59: 905–911.

4. Sorimachi H, Imajoh-Ohmi S, Emori Y et al. Molecular cloning of a novel mammalian calcium-dependent protease distinct from both m- and mu-types. Specific expression of the mRNA in skeletal muscle. J Biol Chem 1989: 264: 20106–20111.

5. Kramerova I, Kudryashova E, Venkatraman G, Spencer MJ. Calpain 3 participates in sarcomere remodeling by acting upstream of the ubiquitin-proteasome pathway. Hum Mol Genet 2005: 14: 2125–2134.

6. Duguez S, Bartoli M, Richard I. Calpain 3: a key regulator of the sarcomere? FEBS J 2006: 273: 3427–3436.

7. Urtasun M, Saenz A, Roudaut C et al. Limb-girdle muscular dystrophy in Guipuzcoa (Basque Country, Spain). Brain 1998: 121 (Pt 9): 1735–1747.

8. Chou FL, Angelini C, Daentl D et al. Calpain III mutation analysis of a heterogeneous limb-girdle muscular dystrophy population. Neurology 1999: 52: 1015–1020.

9. Richard I, Roudaut C, Saenz A et al. Calpainopathy – a survey of mutations and polymorphisms. Am J Hum Genet 1999: 64: 1524–1540.

10. Krahn M, Bernard R, Pecheux C et al. Screening of the CAPN3 gene in patients with possible LGMD2A. Clin Genet 2006: 69: 444–449.

11. Fanin M, Fulizio L, Nascimbeni AC et al. Molecular diagnosis in LGMD2A: mutation analysis or protein testing? Hum Mutat 2004: 24: 52–62.

12. Piluso G, Politano L, Aurino S et al. The extensive scanning of the calpain-3 gene broadens the spectrum of LGMD2A phenotypes. J Med Genet 2005: 42: 686–693.

13. Saenz A, Leturcq F, Cobo AM et al. LGMD2A: genotype–phenotype correlations based on a large mutational survey on the calpain 3 gene. Brain 2005: 128: 732–742.

14. Thiel CT, Kraus C, Rauch A et al. A new quantitative PCR multiplex assay for rapid analysis of chromosome 17p11.2-12 duplications and deletions leading to HMSN/HNPP. Eur J Hum Genet 2003: 11: 170–178.

15. Livak K. Comparative Ct method. ABI Prism 7700 Sequence Detection System. User bulletin. Foster City: PE Applied Biosystems, 1997: 11–15.

16. Leiden Muscular Dystrophy pages© http://www.dmd.nl

17. Ravulapalli R, Garcia Diaz B, Campbell RL, Davies P. Homodimerization of calpain 3 penta-EF-hand domain. Biochem J 2005: 388: 585–591.

18. Stehlikova K, Zapletalova E, Sedlackova J et al. Quantitative analysis of CAPN3 transcripts in LGMD2A patients: involvement of nonsense-mediated mRNA decay. Neuromuscul Disord 2007: 17: 143–147.

19. Richard I, Brenguier L, Dincer P et al. Multiple independent molecular etiology for limb-girdle muscular dystrophy type 2A patients from various geographical origins. Am J Hum Genet 1997: 60: 1128–1138.

20. de Paula F, Vainzof M, Passos-Bueno MR et al. Clinical variability in calpainopathy: what makes the difference? Eur J Hum Genet 2002: 10: 825–832.

21. Frischmeyer PA, Dietz HC. Nonsense-mediated mRNA decay in health and disease. Hum Mol Genet 1999: 8: 1893–1900.

22. Maquat LE. Nonsense-mediated mRNA decay: splicing, translation and mRNP dynamics. Nat Rev Mol Cell Biol 2004: 5: 89–99.

23. Kerr TP, Sewry CA, Robb SA, Roberts RG. Long mutant dystrophins and variable phenotypes: evasion of nonsense-mediated decay? Hum Genet 2001: 109: 402–407.

24. Resta N, Susca FC, Di Giacomo MC et al. A homozygous frameshift mutation in the ESCO2 gene: evidence of intertissue and interindividual variation in Nmd efficiency. J Cell Physiol 2006: 209: 67–73.

25. Hermanova M, Zapletalova E, Sedlackova J et al. Analysis of histopathologic and molecular pathologic findings in Czech LGMD2A patients. Muscle Nerve 2006: 33: 424–432.

26. Pollitt C, Anderson LV, Pogue R et al. The phenotype of calpainopathy: diagnosis based on a multidisciplinary approach. Neuromuscul Disord 2001: 11: 287–296.

27. Todorova A, Georgieva B, Tournev I et al. A large deletion and novel point mutations in the calpain 3 gene (CAPN3) in Bulgarian LGMD2A patients. Neurogenetics 2007: 8: 225–229.

28. Joncourt F, Burgunder J, Steinlin M, Gallati S. LGMD2A caused by a large deletion: clinical, histochemical and molecular analysis. Eur J Hum Genet 2003: 11 (Suppl. 1): 667.

29. Casilli F, Di Rocco ZC, Gad S et al. Rapid detection of novel BRCA1 rearrangements in high-risk breast-ovarian cancer families using multiplex PCR of short fluorescent fragments. Hum Mutat 2002: 20: 218–226.

30. Schouten JP, McElgunn CJ, Waaijer R et al. Relative quantification of 40 nucleic acid sequences by multiplex ligation-dependent probe amplification. Nucleic Acids Res 2002: 30: e57.